LIST OF CHANGES REQUIRED

1. Recent literatures have been included in the Introduction section to support new development related to laser cladding on Ti-6Al-4V alloy (See refs. 5-6). However, relevant references include recent studies on the use of Ti-6Al-4V and not titanium alloys in general.
2. Figs. 2, 3 and 4 have been revised and labelled ((a) and (b)) for clarity.
3. English has been revised on the manuscript.

Influence of ZrB_2 Addition on Microstructural development and Microhardness of Ti-SiC Clad coatings on Ti6Al4V Substrate

Farotade GA[1,*], Popoola API[1] and Pityana SL[2]

[1]Department of Chemical, Metallurgical and Materials Engineering, Faculty of Engineering and Built Environment, Tshwane University of Technology, Pretoria, South Africa, 0001.

[2] National Laser Centre, Council for Scientific and Industrial Research, Pretoria, South Africa,

Abstract

The microstructural features and microhardness of ZrB_2 reinforced Ti-SiC coatings on Ti-6Al-4V substrate were studied.The deposition of these coatings was achieved via laser cladding technique. A 4.0 KW fiber delivered Nd: YAG laser was used to deposit the coatings on the titanium substrate at a laser power of 700 W and laser scan speed of 0.8 m/min. An initial Ti-SiC coating was deposited with no ZrB2 addition followed by deposition of two other coatings with the incorporation of ZrB2 powder at 5 % and 10 % wt. The coatings were examined using scanning electron microscope (SEM) coupled with Energy dispersive spectroscopy (EDS). SEM images of Ti-SiC-ZrB_2 coatings revealed good metallurgical bond between the coatings and the substrate, and also, a significant increment in dendritic formation and inter-dendritic eutectics during solidification within the α-Ti matrix, exhibiting the presence of newly formed phases as the weight percentage of ZrB_2 increased. Back scattered electron (BSE) images also showed the dissolution effect of SiC particles, as the particle-matrix bond strength is influenced by ZrB_2 addition. Furthermore, the microhardness of the Ti-SiC coating was enhanced with increasing ZrB_2 weight percentage. XRD analysis revealed dominant compounds formed during laser material processing. This study deepens the knowledge of possible microstructural features associated with Ti-SiC-ZrB2 cermet coatings.

Keywords: Ti-SiC-ZrB_2 cermet coatings; Microstructure; Microhardness; Laser cladding; Ti-6Al-4V titanium alloy.

1.0.Introduction

In recent times, titanium alloys have been widely utilized in the industrial lines of practice. Ti-6Al-4V alloy covers over 50 % of the most used titanium alloys in these industries, owing to its high strength-to-weight ratio and good resistance to corrosion [1-3]. This elevates its demand based on performance and reliability requirements. Furthermore, due to the presence of α+β phase within its structure, there is a vast variety of microstructures and corresponding properties that can be achieved [4]. For instance, Ding et al. [5] studied the effect of friction stir processing on the phase transformation and microstructure of TiO_2-compounded Ti-6Al-4V alloy. Result showed that the use of Ti-6Al-4V via surface modification is possible with a better performance in biomedical applications. Fiorucci, Lopez and Ramil [6] worked on surface modification of Ti-6Al-4V by nano second laser ablation for biomedical purposes. The authors examined the effect of this process on the biocompatibility of Ti-6Al-4V alloy and found that a micro rough surface of TiO_2 can significantly improve the biocompatibility properties of the alloy texture. However, Ti-6Al-4V alloy possesses low hardness and high susceptibility to oxidation, in effect, limiting its viability in high temperature applications [7-10]. Notwithstanding, this alloy has essential bulk properties which are useful in various applications and a possible solution to its limitations is to protect the surface from being exposed to stringent high temperatures. Laser cladding is a form of surface modification technique that proffers the unique quality of creating refined surfaces with enhanced microstructure and improved thermo-mechanical properties based on ultra-high localized energy intensity. In addition, low thermal effect on base metal with low dilution is observed while minimum level of porosity is also associated with this technique [11].

As Laser cladding proves to be an effective technique in fabricating a wide variety of materials, it can also be employed to develop metal-ceramic coatings which exhibit outstanding performances [12, 13]. This laser surface technique is an effective method where hard particles such as carbides, nitrides and borides can be formed as Ti-based composite clad layers on titanium alloys [14]. Recent studies on surface modification via laser cladding technique on Ti-6Al-4V have been achieved. Fluoroapatite/Zirconia composite coatings have been fabricated on Ti-6Al-4V substrate to replace the conventional use of HA coatings for biomedical implants using laser cladding [15]. In-situ formation of TiC particles have been synthesized by depositing Nickel and graphite on Ti-6Al-4V substrate via laser cladding [16]. Furthermore, the laser cladding of γ-TiAl intermetallic alloys on Titanium alloy has also been achieved [17]. Ti-SiC coating is a prospective candidate for the required improvement of hardness, tribological [18] and oxidation properties of Ti-6Al-4V alloy. It has been reported that Ti-Si-C-B

containing coatings proffer integral excellent properties, produce unique ceramic phases of increased hardness values with several strengthening influence as a result of the enormous attraction among these elements [19-21]. The presence of Boron in coatings can refine the microstructure [22] and also increase the melting efficiency of hard SiC particles owing to the presence of a eutectic phase at 3.6 %B [11]. Moreover, TiSiC-Zr coatings have been observed to yield improved hardness and tribological behavior [23]. Therefore, this work focuses on the effect of ZrB_2 addition to laser clad Ti-SiC coatings on Ti-6Al-4V substrate by examining the microstructure and microhardness of the coatings.

2.0.Experimental Procedure

2.1.Material Preparation

Commercially pure titanium (CP-Ti) powder (45-90 microns) was obtained from TLS, Germany, SiC powders of same mean particle size were ordered from Weartech (Pty) Ltd., South Africa while ZrB_2 powder with average particle size of 10-20 microns was purchased from H.C. Starck GmbH, Germany. The Ti6Al4V substrates with 99.6% purity were also ordered from TLS, Germany. Table 1 shows the chemical composition of the ZrB_2 powder.

The powders were effectively mixed via a Turbula shaker mixer at a mixing speed of 49 rpm for 6 h. With a 200ml cylindrical – shaped plastic container filled to an approximate value of 50 % powder level, the container was placed in the mixing cavity and, then, subjected to translational and rotational motions simultaneously for homogeneity of powders to be achieved. In addition to this, an enhancement of powder flowability was obtained and also to avoid agglomeration which may result to irregular mobility of the powders during laser deposition.

With a dimension 70 x70 x 5 mm, the Ti6Al4V substrates were sandblasted using a jet velocity SiO_2 particles to eliminate surface oxides. The substrates are, then, degreased with acetone and completely dried. This is performed to improve the absorptivity of laser interaction.

2.2.Laser Processing

A 4.0 KW fiber delivered Nd: YAG laser with coaxial nozzles carried and controlled by Kuka robot was used to deposit admixed Ti-ZrB_2 powders on the substrate at the National Laser Centre, Centre for Scientific and Industrial Research (CSIR). Two different compositions were applied; 5 and 10 wt. % ZrB_2. The powder was deposited through argon gas in order to prevent oxidation during deposition. A schematic representation of the laser cladding process is shown in Fig. 1 while the laser parameters set for powder deposition are shown in Table 2.

2.3. Metallographic Examination

The clad samples were longitudinally sectioned using titanium blade cutter, a 350-SiO_2 grit sand paper was used for rough grinding, 800-SiO_2 grit sand paper for fine grinding, while polishing was achieved by using 1 μm Diamaxx Mono polishing paste. The samples were then washed and dried. Furthermore, samples were etched with Kroll's reagent in order to observe distinct microstructural features.

2.4. Microhardness

The hardness was performed on the samples both transversely and longitudinally. A Matsizawa Seiki MH-5 Vickers microhardness tester was employed. Hardness was performed on each sample from a starting point of 100 μm away from the free surface of the coating to the substrate region thereby applying ten indentations on the longitudinally sectioned surface of the deposited composite to the substrate at an interval of 100 μm. A load of 100 g and a dwell time of 10 seconds were used throughout the hardness test.

3.0.Results and Discussion

3.1.SEM Microstructural Examination

Fig. 2a shows the microstructural interface of laser deposited Ti-SiC coating (thickness of 570 μm) on Ti-6Al-4V substrate, exhibiting a good metallurgical bond. Fig. 2b presents the view of fine dendrites with secondary arms, appearing in form of spheroids, seen along the coating as the depth increases towards the substrate. The dendrites are proofs of an effective dissolution of injected powders and development of new phases within the coating. The SiC particles are distinctively observed within the coating as dark irregular shaped bodies. This is an indication of insufficient laser irradiation to completely melt the particles. As the laser beam radiates towards the substrate, the shiny surface of the substrate reflects a substantial portion of the laser beam, reducing the useful energy needed to melt hard SiC particles [24]. Also, SiC is a refractory material with an extremely high melting point (~2,730°C), therefore the particles have the tendency to absorb the radiant energy to a great extent. Owing to the existence of attached dendrites around the SiC particles, there is a possibility of partial dissolution of SiC particles at the particle boundaries, giving rise to formation of hard secondary phases such as TiC [25].

Fig. 3 is a micrographic view of interfacial zone of 5% ZrB_2 reinforced Ti-SiC coating with an average thickness of 471 μm. The coating exhibited no cracks with uniform transition pattern towards the

substrate. Light colored inter-dendritic and dendritic structures are widely distributed within the matrix of the coating (Fig. 3b) as a result of inclusion of ZrB_2. The dendrites are noticed to be densely populated showing an increase in compositional segregation and formation of new compounds. This also gives an enhanced effect on the metallurgical bond strength [26]. The surfaces of the SiC particles are observed to possess a degree of roughness which was not observed in the coating fabricated with no ZrB_2 addition. There are two possibilities two this phenomenon; kinetic roughening as a result of larger Zirconium atoms or ions and larger momentum of these atoms or ions than titanium atoms within the structure [23]. Another possible rationale can be linked with the high boron affinity for carbon, depleting the un-melted SiC particles of carbon. This leads to the formation of hard compound of B_4C. According to Pei et.al [25], cellular dendrites are formed around the SiC particles as these particles serve as heterogeneous preferred sites for nucleation and rapid solidification of non-equilibrium hard phases. Therefore, multiple strengthening effects result from the formation of these various intermetallic phases that can be seen from the x-ray diffraction analysis of the coating.

Fig. 4a shows the microstructure of 10 %ZrB_2 reinforced Ti-SiC laser cladding coating. A well-defined metallurgical bond can be observed between the clad and the substrate. There is a dominant feature of densely populated dendrites at the mid-region of the coating while the transition region is characterized by columnar dendrites depicting the chilling direction towards the substrate during solidification. Densely populated dendritic grains are observed with random growth directions in Fig. 4b. These growth directions are associated with the multiple directions of heat transfer conditions within the coating matrix [27]. Rough surfaces of SiC particles are also noticed in the coating matrix (Fig. 4a). Furthermore, as the ZrB_2 content increases, there is an underlying growth of eutectics interwoven with the dendrites, thus, kinetic efficiency for component segregation is encouraged to form more secondary phases.

3.2.Back scattered electron (BSE) image micro-analysis

The distinctive features observed in Fig. 5 proves the intense reaction that occurs as SiC particles are deposited in the melt pool during laser processing. Laser cladding is known to be portrayed as a process that undergoes rapid rate of cooling with enormous temperature gradients such as 3200°C-1600°C, resulting to formation of non-equilibrium multi-compositional phases around the SiC particles. The pink colored sections, labelled as the rim, contain carbon-rich compounds. The elemental composition of this section can be seen in Table 3. Close to the free surface of the coating, compound dendrites are realized,

depicting the high precipitation of hard carbon phases. There is a downward gradient in mass fraction of the dendrites as depth increases. This is also an indication of high hardness values of Ti-SiC coatings.

In comparison with coating deposited with no ZrB_2 addition, the mass fraction of the rim section of Ti-SiC-10 %ZrB_2 coating is reduced as ZrB_2 is incorporated in the coating (Fig. 6). This observation could be related to the fluxing ability of boron on the dissolution of SiC particles by reducing the melting temperature of the hard particles. Also, formation of brittle polycrystalline TiC within the rim section tend to reduce the interaction strength between SiC particles and the matrix [25], increasing the instability within the coating when it is subject to stress. Therefore, a reduction in the formation of polycrystalline TiC as the rim volume decreases, will encourage a stronger bond strength at the particle-matrix interface and a corresponding increase in dispersed B_4C within the coating matrix. Therefore an increase in ZrB_2 promotes the particle-matrix bond strength and also increase precipitation strengthening effect within the coating.

3.3.Microhardness Analysis

The microhardness chart of the laser based coatings reveals the effect of ZrB_2 addition to the Ti-SiC composition (Fig. 7). With no ZrB_2 addition, the microhardness value of the coatings maintains an average value of 1115.9 HV which is significantly lower than the values of 5 % and 10 % ZrB2 reinforced coatings (1375.4 HV and 1396.7 HV respectively). The profile also shows the reality of the increased hardness value with the application of coating to a depth of about 700 μm, followed by the transition region where microhardness value decreases progressively towards the substrate. The reason for the rise in hardness as the weight percentage of ZrB_2 increases is because of the tendency of ZrB2 particles to increase the degree of dislocation build up during solidification. Consequently, there is a corresponding increase in restriction to plastic deformation resulting in improved hardness of the coating [28].

3.4.XRD Analysis

The present phases on the coatings are analyzed in order to relate their combined effects on the substrate. Fig. 8 displays the XRD patterns of the ZrB_2 reinforced Ti-SiC coatings. Dominant peaks reveals hard phases such as Zr_3C_2, Ti_5Si_3, TiB, and Al_2Zr3. The presence of SiC depicts the insufficiency of laser energy to completely melt the particles as only the outer surface of the particles are engaged in reactions to develop the novel phases. Zr_3C_2 displays the highest value of counts may be due to the ease of transition metals to form stable carbide structures when they come in contact with carbon at high

temperatures [29]. Intermetallic Ti_5Si_3 has been reported in the work of [23]. These phases are stable and are hard in nature, a rationale for the improved microhardness of Ti-SiC-ZrB_2 cermet coating. When the weight fraction of ZrB_2 increases (Fig. 8) more phases are noticed such as B_4C, $Si_3Ti_2Zr_3$ and Ti_5Si_4 are formed. In addition, polycrystalline TiC can also be observed among the dominant phases, exhibiting an increase in dissolution potency of the SiC particles, thereby strengthening the coating. This may be a reason for the trend observed with the microhardness of the coatings in Fig. 7.

4.0.Conclusion

This study brings forth an insight into the microstructural features involved in Ti-SiC coatings as ZrB_2 powder is added in fractions of 5 % and 10 %wt. The coatings were deposited at laser power of 700 W and a laser scan speed of 0.8 m/min. Also the microhardness of the coatings were considered while present phases were also included. The following conclusions were derived from this study:

[1]. The coatings formed good metallurgical bonds with no cracks or pores observed, which exhibits one of the unique qualities of laser cladding technique.

[2]. Fine dendrites with secondary arms were observed within the coatings. This displays active dissolution of injected powders and formation of novel phases within the coating. Also, mass fraction of dendrite arms reduced with increasing coating depth as a result of diminishing heat energy with increasing depth during laser-material processing.

[3]. An increase in weight fraction of ZrB_2 there was an increase in compositional segregation and formation of new compounds, also, mass fraction of inter-dendritic eutectics increased with ZrB_2 addition

[4]. SiC particles displayed partial dissolution due to insufficient laser energy. However, undissolved particles aid in the combined resistance to indentation with newly formed hard phases such as Zr_3C_2, Ti_5Si_3, TiB, Al_2Zr_3, B_4C, $Si_3Ti_2Zr_3$ and Ti_5Si_4, resulting to multiple strengthening effect and increase in microhardness.

Acknowledgement

The authors are pleased to acknowledge the technical supports from Tshwane University of Technology, Pretoria, South Africa, and the Council of Scientific and Industrial Research Centre, South Africa. Financial funding from the National Research Foundation, South Africa is highly appreciated.

References

[1]. Mao, Y. S., Wang, L., Chen, K. M., Wang, S. Q. and Cui, X. H. (2013) Tribo-layer and its role in dry sliding wear of Ti-6Al-4V alloy, *Wear, 297*, pp. 1032-1039.

[2]. Chen, C. C. and Wang, C. M. (2014) Effects of Hydrogen loading and type of titanium hydride in grain refinement and mechanical properties of Ti-6Al-4V, *Journal of Alloys and Compounds, 601*, pp. 274-279.

[3]. Carcel, B., Serrano, A., Zanobrano, J., Amigo, V. and Carcel, A. C. (2014) Laser cladding of TiAl intermetallic alloy on Ti6Al4V. Process optimization and properties, 8th International Conference on Photonic Technologies LANE 2014, *Physics Procedia, 56*, pp. 284-293.

[4]. Velga, C., Davim, J. P. and Loureiro, A. J. R. (2012) Properties and applications of titanium alloys: A brief review, *Review of Advanced Materials Science, 32(2)*, pp. 133-148.

[5]. Ding, Z., Zhang, C., Xie, L., Zhang, L. C., Wang, L. and Lu, W. (2016) Effect of friction stir processing on the phase transformation and microstructure of TiO2-compounded Ti-6Al-4V alloy. *Metallurgical and Materials Transactions A, 47(12)*, pp. 5675-5679.

[6]. Fiorucci, M. P., Lopez, A. J. and Ramil, A. (2015) Surface modification of Ti-6Al-4V by nano second laser ablation for biomedical applications. *In Journal of Physics: Conference Series (Vol. 605, No. 1, pp. 012022)* IOP Publishing.

[7]. Razavi, G., Zirepour, G., Saboktakin, M. and Monataji, H. (2011) Investigation of enhancing surface hardness in Ti-6Al-4V alloy by TIG welding, In proceeding of 2011 International conference on Advanced Materials Engineering (ICAME 2011).

[8]. Morita, T., Asakura, K. and Kagaya, C. (2014) Effect of combination treatment on wear resistance and strength of Ti-6Al-4V alloy, *Materials Science and Engineering A, 618*, pp. 438-446.

[9]. Lin, Y. C., Chen, H. M. and Chen, Y. C. (2014) The effect of different methods to add nitrogen to titanium alloys on the properties of titanium nitride clad layers, *Material Design, 54*, pp. 222-229.

[10]. Tiang, H., Wang, Y. M., Zhang, Y. F., Guo, L. X., Ouyang, J. H., Zhou, Y. and Jia, D. (2015) Oxidation resistance of $AlPO_4$ bonded ceramic coating formed on titanium alloy for high temperature applications, *International Journal of Applied Ceramic Society, 12(3)*, pp. 614-624.

[11]. Molnar, A., Buza, G. and Balogh, A. (2013) Hardness test and microstructure analysis of NiCrBSi sprayed laser remelted coatings, *Production Processes and Systems, 6(1)*, pp. 35-46.

[12]. Zhang, K. M., Zou, J. X., Li, J., Yu, Z. S. and Wang, H. P. (2012) Synthesis of Y_2O_3 particle enhanced Ni/TiC composite on TC4 Ti alloy by laser cladding, *Transitional Non-ferrous Metallurgy Society of China*, *22*, pp. 1817-1823.

[13]. Ochonogor, O. F., Meacock, C., Abdulwahab M., Pityana, S. and Popoola, A. P. I. (2012) Effect of Ti and TiC ceramic powder on laser-cladded Ti-6Al-4V in situ intermetallic composite, *Applied Surface Science, 263*, pp. 591-596.

[14]. Vilar, R. (2014) Laser powder deposition, In Hashmi, S. (ed), *Comprehensive Materials Processing, 10*, pp. 163-216.

[15]. Chien, C. S., Liu, C. W. and Kuo, T. Y. 2016. Effects of laser power on microstructural properties and phase composition of laser-clad Fluoroapatite/Zirconia composite coatings on Ti-6Al-4V substrate, *Materials, 9*(5), pp. 380.

[16]. Liu Y., Ding, J., Qu, W., Su. Y. and Yu, Z. 2017. Microstructure evolution of TiC particles in situ, synthesized by laser cladding, *Materials, 10*(3), pp. 281.

[17]. Maliutina, I. N., Si-Mohand, H., Piolet, R., Missemer, F., Popelyukh, A. I., Belousova, N. S. and Bertrand, P. 2016. Laser cladding of γ-TiAl intermetallic alloy on titanium alloy substrates, Metallurgical and Materials Transactions A, 47(1), pp. 378-387.

[18]. Munteanu, D., Ionescu, C., Olteanu, C., Munteanu, A., Davin, F., Cunha, L.,Moura, C. and Vaz, F. (2010) Influence of composition and structural properties in the tribological behavior of magnetron sputtered Ti-Si-C nanostructured thin films, prepared at low temperature, *Wear, 268(3-4)*, pp. 552-557.

[19]. Tian, Y. S., Chen, C. Z., Chen, L. B., Liu, J. H. and Lei, T. Q. (2005) Wear properties of alloyed layers produced by laser surface alloying of pure titanium with B_4C and Ti mixed powders, *Journal of Material Science, 40*, pp. 4387-4390.

[20]. Das, M., Balla, V. K., Bascu, D., Bose, S. and Bandyopadhyay, A. (2010) Laser processing of SiC-particle-reinforced coating on titanium, *Scripta Materialia, 63*, pp. 438-441.

[21]. Krakhmalev P. and Yadroitsev, L. (2014) Microstructure and properties of intermetallic composite coatings fabricated by selective laser melting of Ti-SiC powder mixtures, *Intermoetallics, 46*, pp. 147-155.

[22]. Islak, S., Ozorak, C., Sezgin, C. T. and Akkas, M. (2016) Effect of boron on microstructure and microhardness properties of Mo-Si-B based coatings produced via TIG process, *Archives of Metallurgy and Materials, 61(3),* pp. 1169-1174.

[23]. Vitelaru, C., Balaceanu, M., Parau, A., Luculescu, C. R. and Vladescu, A. (2014) Investigation of nanostructured TiSiC-Cr hard coatings for industrial applications, *Surface and Coating Technology, 251*, pp. 21-28.

[24]. Sateesh, N. H., Kumar, G. C. M. and Krishna, P. (2015) Influence of Ni-P coated SiC and laser scan speed on the microstructure and mechanical properties of IN625 metal matrix composites, *Lasers Manufacturing and Materials Processing, 2*, pp. 187-198.

[25]. Pei, Y. T., Ocelik, V. and De Hosson, J. Th. M. (2002) SiC_p/Ti6Al4V functionally graded materials produced by laser melt injection, *Acta Materialia, 50*, pp. 2035-2051.

[26]. Amigo, V., Candel, J. J. and Franconetti, P. (2012) Titanium metal matrix composite laser coating based on carbides, *Material Science Forum, 727-728*, pp. 299-304.

[27]. Guo, H. M., Wang, Q., Wang, W. J., Guo, J., Liu, Q. Y. and Zhu, M. H. (2015) Investigation on wear and damage performance of laser cladding Co-based alloy on single wheel or rail material, *Wear, 328-329,* pp. 329-337.

[28]. Dinaharan, I., Murugan, N. and Parameswaran, S. (2011) Influence of in situ formed ZrB2 particles on microstructure and mechanical properties of AA6061 metal matrix composites, *Material Science and Engineering A, 528*, pp. 5733-5740.

[29]. Zhong, Y., Xia, X., Shi, F., Zhan, J., Tu, J. and Fan, H. J. (2016) Transition metal carbides and nitrides in energy storage and conversion, *Advanced Science, 3(5),* 1500206.

TABLES

Table I: Chemical Composition of ZrB_2 powders

S/N	Compositional Content	Percentage Composition (%)
1.	Zirconium diboride (ZrB_2)	96-97
2.	Hafnium diboride (HfB_2)	0.2-2.5
3.	Diboron trioxide (B_2O_3)	< 1

Table II: Laser Parameters for Deposition of Ti-SiC-ZrB_2 Cermet Coatings

S/N	Composition	Laser Power (W)	Laser Scan Speed (m/min)	Laser Beam Size (mm)	Gas flow rate (L/min)	Powder feed rate (rpm)
1	Ti-20%SiC-5%ZrB_2	700.0	0.8	3.0	1.2	1.0
2	Ti-20%SiC-10%ZrB_2	700.0	0.8	3.0	1.2	1.0

Table III: Semi-quantitative Energy Dispersive X-ray Micro-analysis

Region/Section	Titanium (%)	Silicon (%)	Aluminium (%)	Zirconium (%)
SiC	0.4-0.9	99.1-99.6	-	-
Rim	92.5-97.2	2.5-4.8	0.5-2.1	0.4-2.1
Upper Matrix	84.4-91.5	2.9-11.9	2.1-2.7	0.5-2.1
Lower Matrix	90.1-95.4	2.3-7.9	2.4-2.8	0.3-1.9
Substrate	94.2-94.9	-	5.1-5.8	-

LIST OF FIGURES

FIGURES

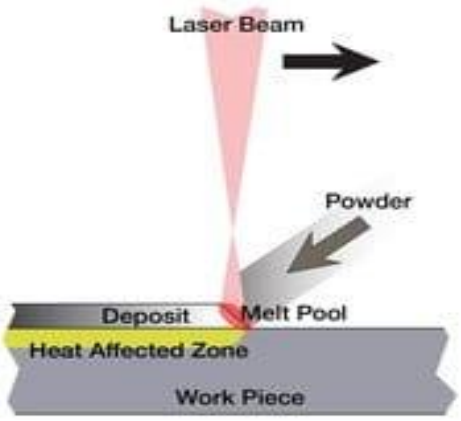

(I)

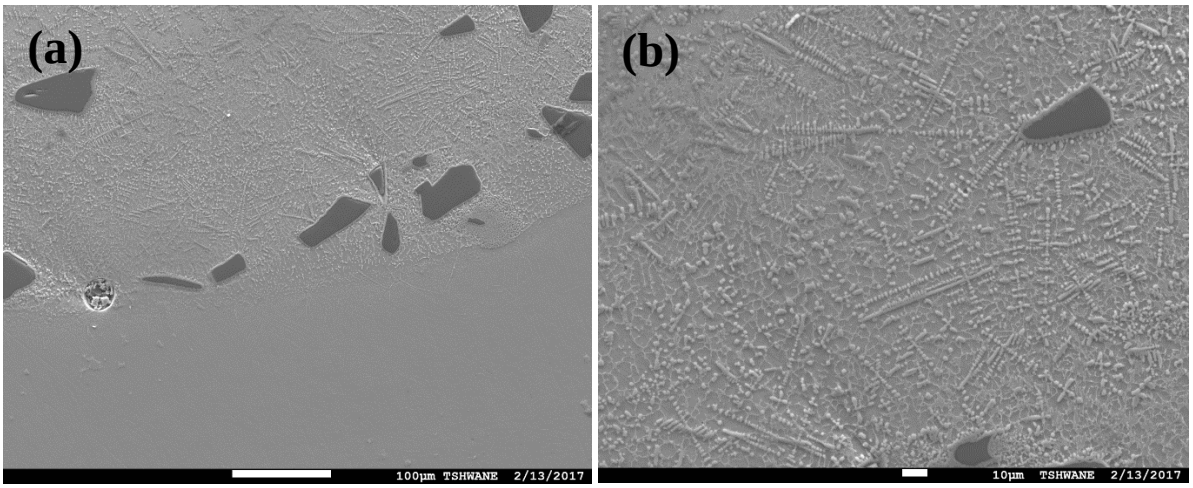

(II)

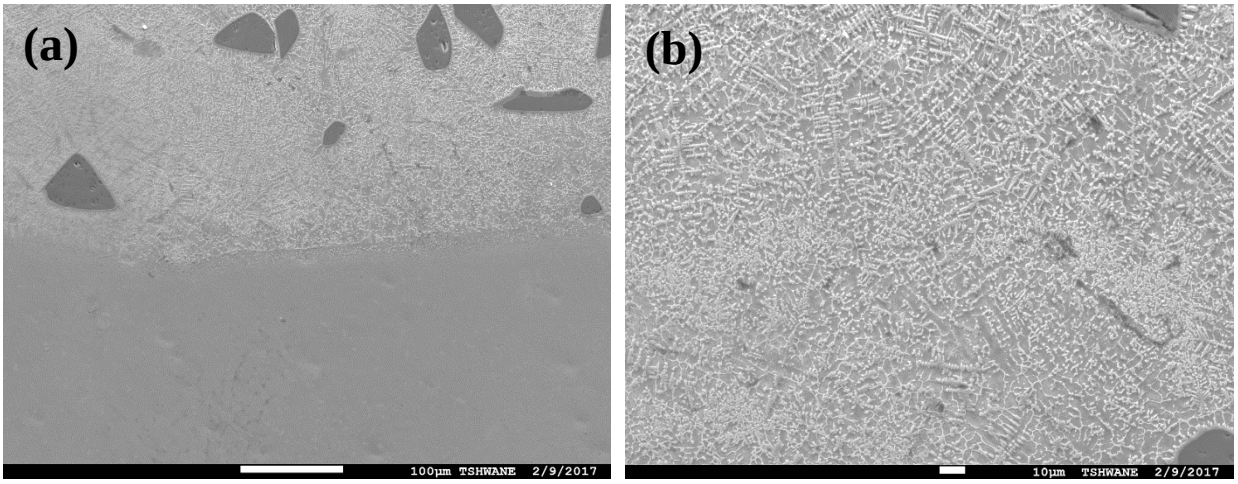

(III)

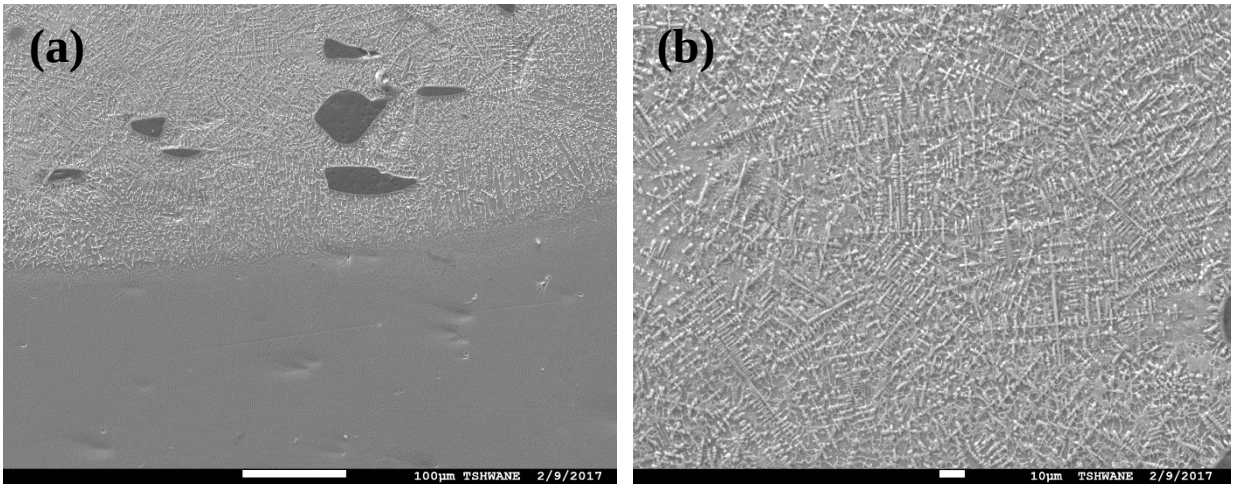
(a)
100µm TSHWANE 2/9/2017
(b)
10µm TSHWANE 2/9/2017

(IV)

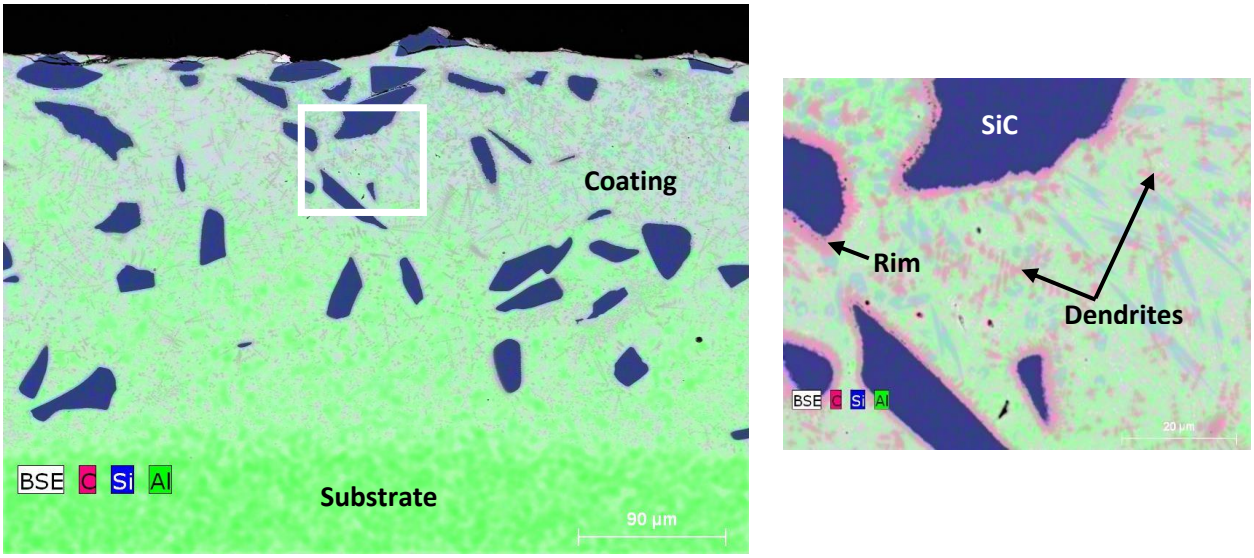
Coating
BSE C Si Al
Substrate
90 µm
SiC
Rim
Dendrites
BSE C Si Al

(V)

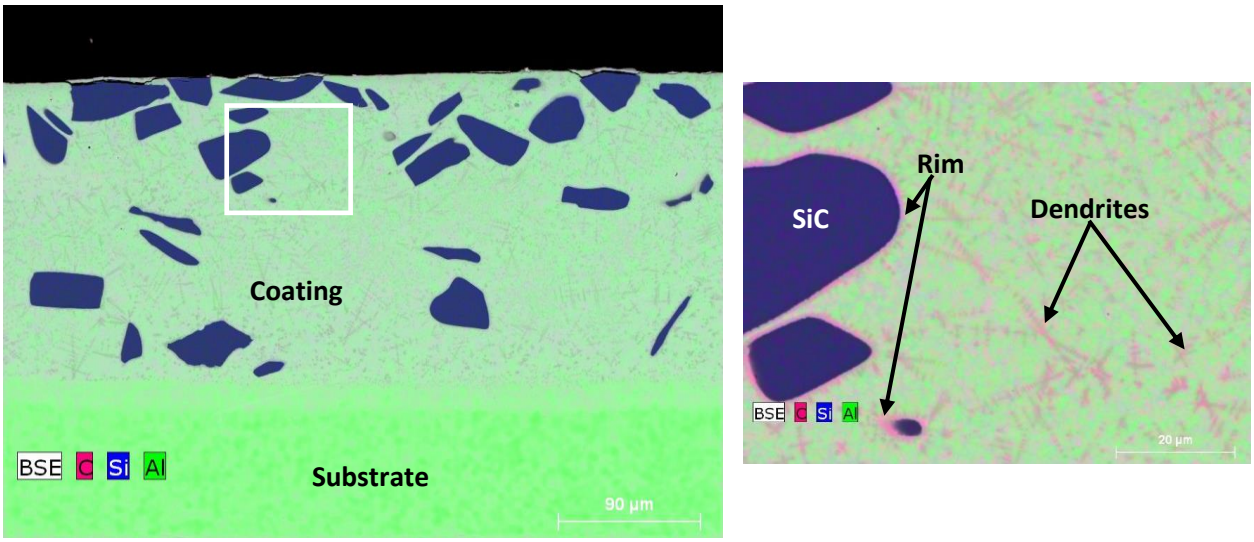
Coating
Substrate
BSE C Si Al
90 µm
SiC
Rim
Dendrites
BSE C Si Al
20 µm

(VI)

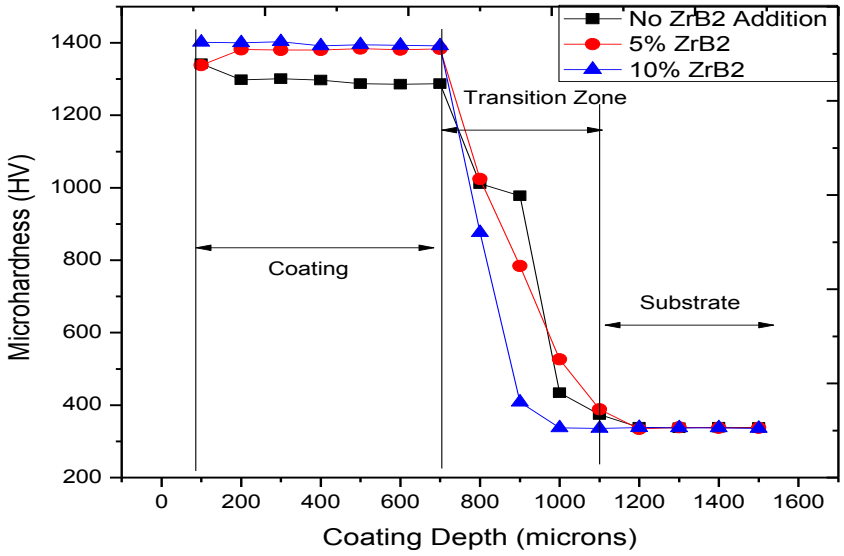
No ZrB2 Addition
5% ZrB2
10% ZrB2
Transition Zone
Coating
Substrate
Microhardness (HV)
Coating Depth (microns)
200
400
600
800
1000
1200
1400
1600

(VII)

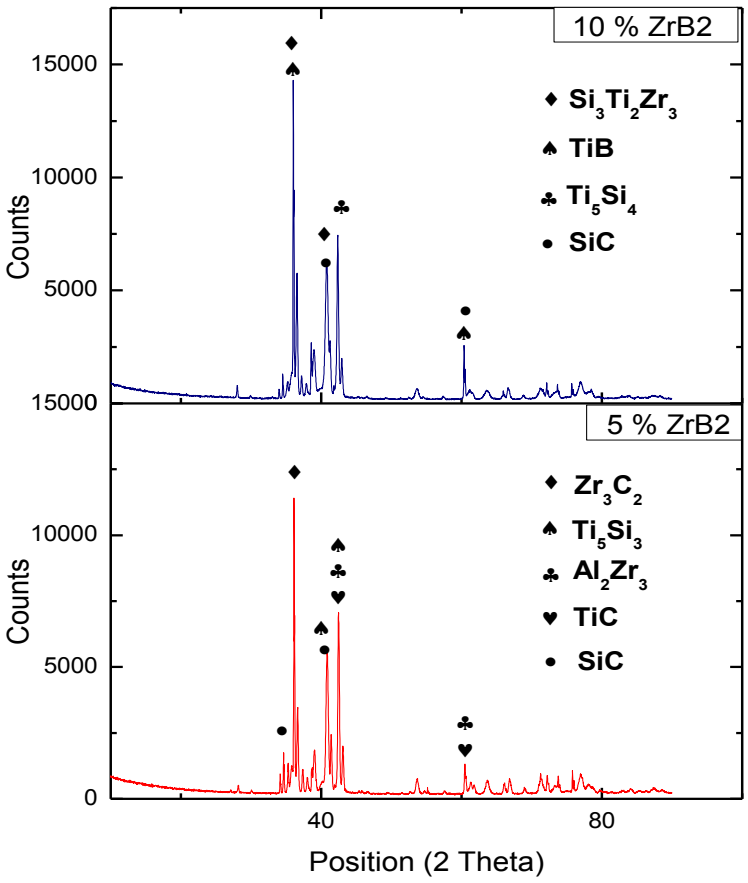
10 % ZrB2
Si3Ti2Zr3
TiB
Ti5Si4
SiC
5 % ZrB2
Zr3C2
Ti5Si3
Al2Zr3
TiC
SiC
Counts
Counts
15000
10000
5000
0
40
80
Position (2 Theta)

(VIII)